

Shake Table Tests to Measure the Dynamic Performance of Geotextile-reinforced Embankment

61 (4), pp. 803–814, 2017

<https://doi.org/10.3311/PPci.10540>

Creative Commons Attribution 

Ayşe Edinçliler^{1,*}, Yasin S. Toksoy¹

RESEARCH ARTICLE

Received 25 January 2017; Accepted 21 February 2017

Abstract

Using geosynthetics in highway embankments can reduce the impact of hazardous earthquakes by transmitting less excitation to improve the seismic performance. This study uses a 1-g reduced scale (1/50) approach and subjects the model embankment to an earthquake time history as well as several levels of uniform cyclic loading. The main focus of comparison is between an unreinforced embankment and a one, reinforced with two levels of geosynthetics material. Results reveal that geotextile reinforced highway embankment models perform much better under the applied motions. Larger amplitudes cause more severe deformations as a result of the increased dynamic loads. It is also revealed that the effectiveness of the geosynthetics is dominated by the seismic frequency. Deamplification is observed within the geotextile reinforced embankment but the degree of deamplification is highly depended on the predominant frequency of the dynamic load.

Keywords

Reinforced highway embankment, seismic performance, shake table experiment, dynamic motion, earthquake, geotextile reinforcement

1 Introduction

Highways are essential lifelines that should be in operation even after disastrous events. For that reason, during and after earthquakes, earth structures such as highway embankments should be stable enough to provide required safety and emergency needs. The stability of slopes, dams, and embankments is a serious problem under static and dynamic loads which should be permanently solved during the construction phases. Thus, engineering applications are required to reinforce embankments and to satisfy the required stability conditions. Geosynthetics or related materials placed under foundations can absorb seismic energy, thus transmit smaller levels of excitation to an overlying structure which can be a cost effective way to mitigate earthquake related hazards on geotechnical structures [1]. In the literature, geosynthetics and tire waste inclusions are used to increase the stability of the highway embankments ([2], [3], [4]). The use of geosynthetics has grown rapidly and today, geosynthetics are commonly used in many of the engineering applications as a reason of the numerous advantages. Geosynthetics have proven to be useful and cost-effective site improvement materials. They have become essential materials in civil engineering and environmental geotechnics. Application of the geosynthetics in highway embankments provides an additional tensile strength and durability to the structures under horizontal and vertical loads and enables engineers to construct more stable and earthquake resistant highway embankments. Geosynthetic reinforced steepened slopes can be constructed with slope face angles up to 70° from horizontal, however typical unreinforced soil slopes are limited to the inclination of 25 to 30° or less, depending on the slope soil [5]. In the literature, the influence of geosynthetics on the dynamic behaviour of geotechnical structures are studied with several shake table and centrifuge testing experiments.

Shake table tests are very useful way to simulate any natural or artificial dynamic motions under laboratory conditions. In the literature, it is possible to find many kinds of different studies on geosynthetic reinforcement of different geotechnical structures. El-Emam and Bathurst ([6], [7]) performed shake table tests to determine the influence of reinforcement design

¹Bogazici University, Kandilli Observatory and Earthquake Research Institute, Department of Earthquake Engineering, Istanbul, Turkey

* Corresponding author email: aedinc@boun.edu.tr

parameters on the dynamic response of retaining walls. In their study, the predominant frequency of the input was used as 5Hz for the 1/6 scaled model. This frequency value corresponds to 2Hz of frequency at the prototype scale according to the scaling laws of Iai [8], which was much lower than the fundamental frequency of the system. Their study revealed that the increase of reinforcement length, stiffness and the number of reinforcement layers reduced the lateral displacements under given dynamic motions.

It is possible to find shake table experiments related to the seismic behaviour of reinforced slopes and embankments. Six steep geosynthetic reinforced slopes were tested on a shake table by Perez and Holtz [9]. Slopes were designed to have an angle of 63° with 1.2 m of height and silica sand was used throughout the study. A frequency of 5 Hz was chosen to determine the seismic behaviour of slopes with different L/H ratios and geosynthetic spacing. Test results showed that both L/H ratio and geosynthetic spacing were essential parameters for geosynthetic reinforced slopes and embankments. During the tests, it was observed that an increase in L/H ratio and decrease in geosynthetic spacing lead to more stabilized models.

A study by Wartman et al. [10] focused on seismically induced deformations in slopes performing shake table tests with the aim of determining the failure mechanisms of slopes under dynamic loading and to investigate the applicability and the accuracy of the Newmark sliding block procedure. Four slopes with different geometric parameters were designed and instrumented in a plexiglas box and tested by shake table under 1g of acceleration. Results of the study showed that all slope models deformed under dynamic loading with deep rotational and translational sliding displacement. In addition, the accuracy of the Newmark method was found to be moderate for dynamic analysis. Seismic slope behaviour was studied in a large-scale shake table model test by Lin and Wang [11]. Using a uniform medium sand, a model slope with dimensions of 0.5 × 1.3m and a slope angle of 30° was created in a plexiglas sided box. The scaling factor used during the experiments was 1/20. Results of the experiments revealed that significant soil amplification was observed especially when non-linear behaviour took place that may influence the failure of the slope and the failure surface was circular and close to the slope surface. The only study in the literature which is related to the effect of frequency on seismic response of reinforced soil slope is given by Srilatha et al. [12]. Clayey soil was used for the experiments. Reinforced and unreinforced slopes were tested using shake table in a laminar box. Biaxial geogrids were used for reinforcement of slopes. Designing two different angles of 45° and 60°, slope models were excited dynamically under 0.3g base acceleration with different frequency values of 2, 5 and 7Hz. It was concluded that the increase in frequency values leads to an increase in displacement values.

Centrifuge modeling is another technique for dynamic testing of the physical scale models of the engineering structures. Numerical and experimental studies were conducted by Yang et al. [13] on geosynthetic reinforced soil slopes. A series of centrifuge tests were performed using a non-woven interfacing fabric reinforcement which has strength parameter of T_{ult} : 0.03kN where Monterey No.30 sand was used as backfill. Centrifuge tests were performed at 50g acceleration and the failure surface was determined. Finite element model of the same model was created using the program ANLOG. The Finite Element Model (FEM) of centrifuge test was performed at 45g. It was determined that both numerical and experimental results verify each other. Aklik and Wu [14] performed centrifuge tests on geosynthetic reinforced slopes. 440x400x155mm size rigid box was used for the experiments. Uniform coarse sand with internal friction angle of 34° was used as the foundation material. Three different slope inclinations of 65°, 75°, and 85° were reinforced with six, seven and eight layers of geotextile and subjected to centrifuge test. In order to investigate amplification and deamplification responses of geosynthetic reinforced slopes, Yang et al. [15] performed a series of dynamic centrifuge tests up to 50g. During the experiments, a variety of input ground motions were used. The effects of input ground acceleration and input motion frequency on the amplification and deamplification responses of slopes are given. It was concluded that acceleration amplification factor is clearly affected by the changes of input ground acceleration. Also, it was determined that acceleration amplification factor is distributed non-uniformly along the height of the geotextile reinforced slope and amplification and deamplification responses increase with the height in the light of the obtained results from centrifuge tests. In addition to that, it was also noted that acceleration responses are very dependent on the seismic frequency.

Scaled shake table tests are commonly used in engineering due to the nature of the shake table load and dimension restrictions, financial aspects and laboratory conditions. Seismic behaviour of the embankments and dams can be observed by using the defined scaling factors in the experimental studies. Typical scale factors for shake table experiments for modelling of the dams up to 1:75 scaling factor for strength models and 1:400 scaling factor for elastic models are given in the literature [16]. Based on the given statements in the literature, various studies with a scaling ratio of 1:50 or even smaller experimental models successfully reflect the typical behaviour of the prototype geotechnical structure. An experimental study by Cihan and Yuksel [17] presents the shake table results of a 1:50 scaled breakwater slope.

Another study by Harris et al. [18] performed a shake table experiment of a 1:50 scaled dam structure. Also, Edinçliler and Güler [2] performed a series of experiment on a 1/100 scale geotextile reinforced embankment model to simulate failure mechanisms during the construction and lifetime of embankments.

In this study, a 1/50 scaled highway embankment model was designed and reinforced with geosynthetics in order to investigate the effect of different dynamic motions with differences in amplitude and frequency domain. Also, the benefits of the geotextile reinforcement compared to unreinforced case are evaluated. Thus, a series of shake table tests were performed for the identical unreinforced and reinforced embankment models designated as UREM and REM, respectively. This study is different from the literature studies because it is concentrated on the effect of amplitude and frequency domain properties on the seismic behaviour of the reinforced embankments with full correlation of the proposed scaling laws. During the experiments, accelerations travelling through the embankment and the vertical and horizontal displacement values for each case were obtained. During the experiments, the slope failure was observed.

2 Material and methods

Experimental design considerations, the details of the shake table model, material properties of embankment fill, foundation soil and the geosynthetic reinforcement, instrumentation and input motions are given in the following parts.

2.1 Design Considerations

Highway embankment models for shake table experiments were designed using a rigid soil box with dimensions of $90 \times 40 \times 50$ cm. The box is made of plexiglas with 15mm thickness. Plexiglas is usually preferred for shake table experiments because the material itself is highly resistant to dynamic and static loads, transparent and rigid enough to perform the model tests [19]. Before conducting the experiments, the performance check of the plexiglas box was evaluated and approved to be available for shake table tests [20]. The shake table tests in this study are 1g model studies carried out on reduced scale models. The stresses and deformations measured in the experiments do not truly represent the stresses and deformations in the field because of low confining pressures and boundary effects in model studies. Establishing scaling rules between the reduced-scale model and the prototype is a major difficulty in shake table testing. Firstly, similitude requirements for the geometry of the embankment, materials, loading and interpretation of results are evaluated. Then, similarity relations for shake table experiments were chosen due to the defined typical scaling factors by Harris and Sabnis [16] and the similitude law of Iai [8]. Of the various suggestions offered in the literature, rules proposed by Iai [8] are widely used to scale the geometry of the model and the properties of the components. These similitude rules for shake table tests conducted in a 1g gravitational field, derived from the basic equations governing equilibrium and mass balance, were adopted in this study to scale down the necessary variables. Reinforcement stiffness, duration and frequency of the dynamic motions are determined with respect

to the proposed requirements considering a scale factor of λ : 50. Table 1 presents the scaling factors given by Iai (1989) and corresponding values in this study.

Table 1 Variables changed due to scaling factors.

Variable	Scale Factor	Experimental Study
Length	λ	50
Density	1	1
Strain	1	1
Strength	1	1
Acceleration	1	1
Frequency	$\lambda^{-0.5}$	$1/\sqrt{50}$
Time	$\lambda^{0.5}$	$\sqrt{50}$

UREM and REM are designed with respect to the regulations and the recommendations of FHWA-NHI-09-083. The prototype highway embankment is considered as a wide, four lane structure and the model embankment is designed as a 1:50 scale of the prototype. All models were placed over the same foundation soil layer with density of 16.5 kN/m^3 and the relative density of Dr: 60%. All embankment models have the same dimensions of H:20cm, L:20cm with the same inclination of 45° . Physical appearance of embankment model can be seen in Fig. 1.

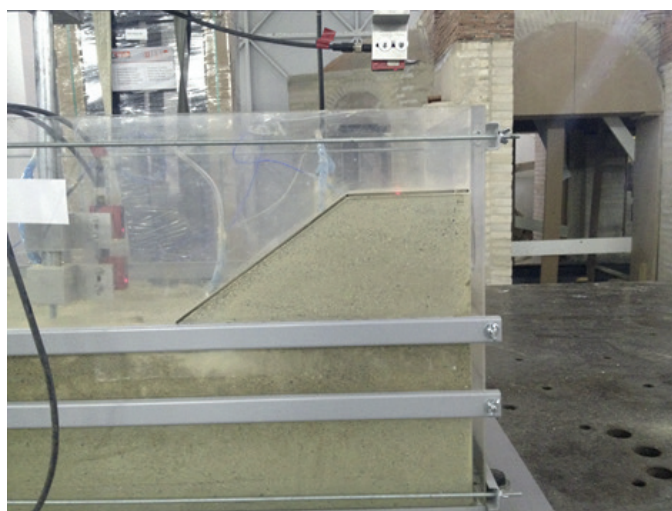


Fig. 1 Physical appearance of the model.

In order to obtain the required number of reinforcement layers and reinforcement parameters, limit equilibrium method was used in the design of the UREM and REM. In addition, preliminary numerical studies were performed to analyse the static and dynamic stability of embankments. Studies showed that two layers of geosynthetic reinforcement can be sufficient for obtaining the required factor of safety [21]. REM includes two layers of reinforcement material, one layer was placed between the bottom of the embankment and the foundation soil and the second layer was placed right in the middle between the crest and the bottom of the embankment. The reinforcement materials are expected to increase the seismic performance of the model.

2.2 Materials

For embankment and foundation soil, the sand material used during the experiments is named as “Silivri Sand” which is locally found around Istanbul region and it is widely used for highway embankments. The grain-size distribution of the sand according to the ASTM Standard of D422 is given in Fig.2. According to the USCS system, the sand material is classified as poorly graded sand (SP) with C_u : 2.29 and C_c : 1.1 [22].

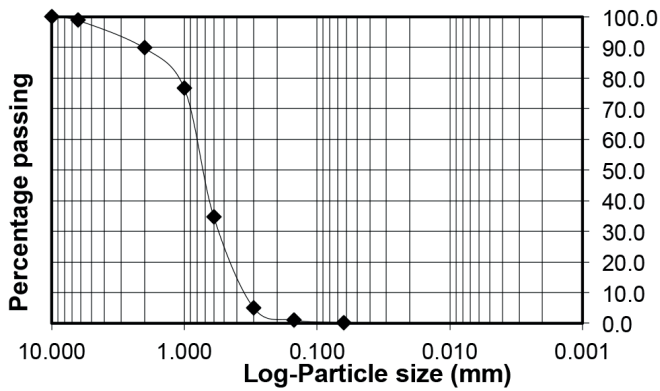


Fig. 2 The grain-size distribution of the sand.

The geotextile used for this study is a woven type geosynthetic material. The geotextile properties used in the experiments is 1/50 times scaled with respect to the scaling laws [8]. Due to the scaling law, the relationship between prototype and reduced scale model reinforcement stiffness are given as follows:

$$J_p = J_m \lambda^2$$

where;

J_p : Prototype scale reinforcement stiffness

J_m : Reduced scale model reinforcement stiffness

λ : Scaling factor

The scaled geotextile has the tensile strength of 0.07 kN/m with a reinforcement stiffness (J_m) of 0.46 kN/m, which is 2500 times weaker than the 1150 kN/m (J_p) of the prototype stiffness. Tests were conducted at Boğaziçi University Soil Mechanics Laboratory under 25°C of temperature and 40% humidity. The maximum elongation of the material at rupture is around 10%. The shear modulus of the sand material, G , was obtained using shear wave velocity. The shear modulus value was found as $G = \rho \cdot V_s^2$

2.3 Instrumentation

A total of nine accelerometers and four displacement sensors were used for the experiments. Accelerometers and displacement sensors are notated with letters of “A” and “D”, respectively. A1 was located on the shake table and measures the input ground motion. A2 was located on the soil box, A3, A4, A5 and A6 were placed inside the sand foundation and were located linearly at the same level. A7 was placed under the first reinforcement layer. A8 was placed between two reinforcement layers inside the embankment and A9 was located

above the second reinforcement layer at the top of the embankment. D1 is a displacement sensor and measures the input displacements. D2, D3 and D4 are laser displacement sensors. D2 measures the displacement at the bottom of the embankment models while D3 measures the displacement at the top of the models. D4 was located to measure the settlement at the top of the embankment models. Instrumentation plan for all models is represented in Fig. 3.

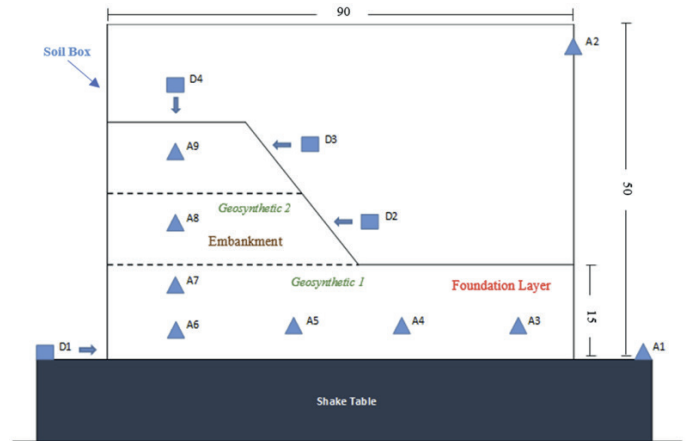


Fig. 3 Instrumentation plan for all embankment models.

2.4 Inputs and methods

Experimental study covers determination of the effects of acceleration amplitude and predominant frequency of the motion on the seismic performance of unreinforced and reinforced embankment models. The influence of the dynamic load parameters on the scaled unreinforced and reinforced highway embankments is evaluated. A series of shake table experiments were performed with using the designed plexiglas soil box. Unreinforced and reinforced embankment models with 45° inclination were prepared inside the soil box. The shear wave velocity of sand material, V_s , is taken as 140 m/s. This shear wave velocity is within the reasonable range of a medium sand. For the embankment model, the resonance frequency is calculated as 175Hz. The frequency range used in the present study is much less than the natural frequency and hence the models are not subjected to resonance. In another words, there is no risk of resonance for the applied dynamic motions. Input dynamic motions consist of sinusoidal base motions of two acceleration amplitudes (0.3g and 0.5g) with four predominant frequencies (2Hz, 5Hz, 7Hz and 14Hz) and a time scaled earthquake record of the 1999 Düzce Earthquake ($M_w=7.2$). Selected motions are given in Fig. 4. It is important that a predominant frequency of 14Hz corresponds to an average earthquake frequency value of 2Hz for the 1/50 scaled embankment model with regards to scale laws of Iai [8]. Similarly, Bathurst and Hatami [23] used the predominant frequency as 2Hz for 1/6 scaled model. Frequencies of 2Hz and 3Hz are representative of typical predominant frequencies of medium to high frequency earthquakes. This frequency value is in the range of the expected

earthquake parameters. The rest of the frequency ranges were used to evaluate the seismic behaviour patterns of the existing embankment models.

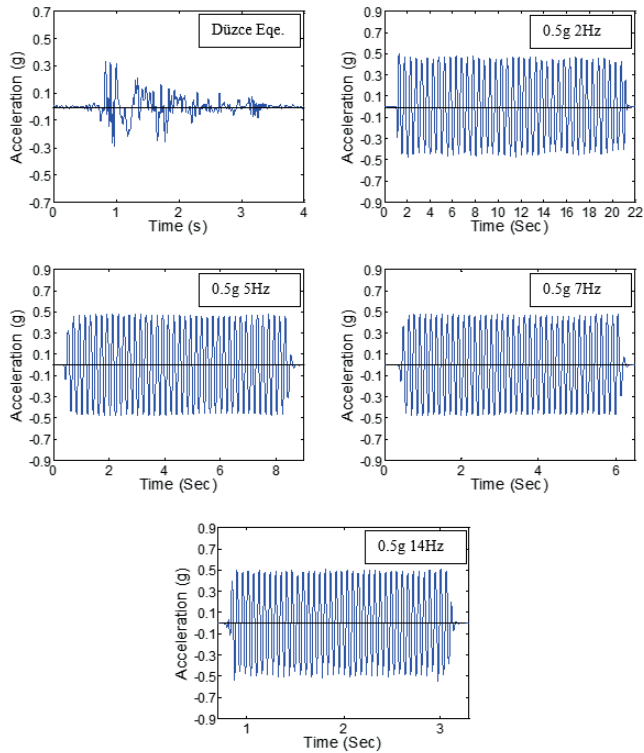


Fig. 4 Selected dynamic motions used during the experiments.

Experimental program consists of 18 different cases subjected to nine different dynamic motions are given in Table 2. The seismic performance of the embankment models was evaluated comparing transmitted acceleration values, spectral accelerations with corresponding period values and the amount of displacements. In addition, Amplification Factor(s) (A.F.) are calculated as the ratio of transmitted maximum acceleration to the peak input acceleration value (PGA). Shake table tests were carried out at Boğaziçi University Kandilli Observatory and Earthquake Research Institute.

Table 2 Experimental program.

Test No:	PGA	Frequency	Reinforcement Type	Number of Cycles
1	0.35	-	Unreinforced	-
2	0.35	-	Geotextile	-
3	0.30	2	Unreinforced	40
4	0.30	5	Unreinforced	40
5	0.30	7	Unreinforced	40
6	0.30	14	Unreinforced	40
7	0.30	2	Geotextile	40
8	0.30	5	Geotextile	40
9	0.30	7	Geotextile	40
10	0.30	14	Geotextile	40
11	0.50	2	Unreinforced	40
12	0.50	5	Unreinforced	40
13	0.50	7	Unreinforced	40
14	0.50	14	Unreinforced	40
15	0.50	2	Geotextile	40
16	0.50	5	Geotextile	40
17	0.50	7	Geotextile	40
18	0.50	14	Geotextile	40

3 Test results and discussion

In this part of the study, measurements which are taken from most critical locations of the models are evaluated. Results are given for the accelerometer A9, which is located between the crest and the second reinforcement layer, and for the transmitted displacement measurements taken from the displacement sensors of D2 and D3. For a better evaluation and comparison, the performed experimental results are tabulated. In order to observe the effects of dynamic motions on seismic performance of the embankment models, base accelerations transmitting through the foundation layer of unreinforced embankment (UREM) and two layered geotextile reinforced embankment (REM) are evaluated. The performance of inclusion of the reinforcement materials on the dynamic behaviour of the REM is evaluated by means of A.F. which are given in Figs.7, 14 and 19.

3.1 Test results under Düzce Earthquake Excitatio

Test results for the 1999 Düzce Earthquake excitation (Test No.1 and 2) are given for both Models in Table 3 and Table 4. Table 3 represents the measured acceleration and Spectral acceleration (SA) values of the embankment model with 45° inclination under the Düzce Earthquake and Fig.5 shows the transmitted acceleration-time histories of the Models.

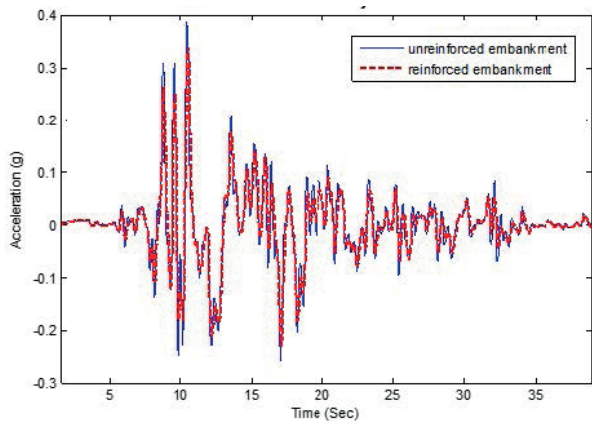


Fig. 5 Acceleration-Time histories of UREM and REM (A9).

As seen in Table 3, under the scaled Düzce Earthquake ground motion, the reinforcement effect is relatively limited. The maximum reduction of the transmitted accelerations is 13% at A9. The measurements of A2–A6 which are located in the foundation soil are close to the input motion.

Table 3 PGA and SA values under the Düzce Earthquake excitations.

	Unreinforced		Reinforced	
	Acc. (g)	SA (g)	Acc. (g)	SA (g)
A1	0.35	1.08	0.35	1.08
A2	0.31	1.08	0.30	1.07
A3	0.24	1.05	0.24	1.05
A4	0.31	1.06	0.30	1.06
A5	0.30	1.07	0.30	1.06
A6	0.31	1.05	0.30	1.05
A7	0.34	1.12	0.32	1.12
A8	0.35	1.13	0.31	1.05
A9	0.39	1.24	0.34	1.14

As shown in Fig. 7, A.F. decreases from 1.11 to 0.97 at the crest of the reinforced model. It shows that inclusion of the geotextile reinforcement deamplifies the transmitted accelerations. Fig. 6 shows the response spectra of UREM and REM.

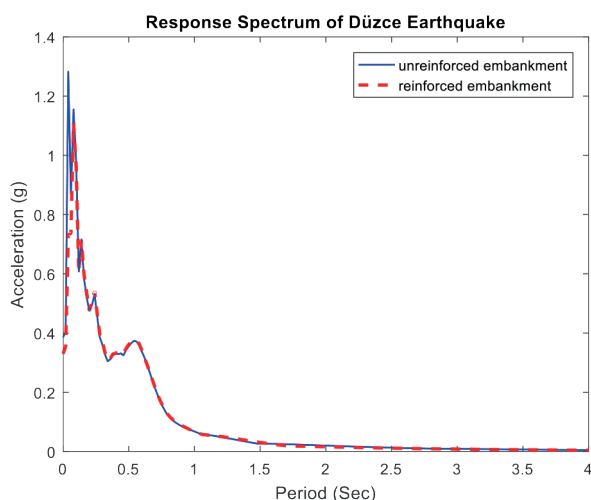


Fig. 6 Response Spectrum under the Düzce Earthquake Excitations for UREM and REM (A9).

As seen in Table 3, tabulated spectral acceleration (SA) values reveal that the effects of geotextile material are clear at A8 and A9 under Düzce Earthquake. For both cases, SA measurements of A2–A6 are very similar to A1, which measures the base excitation and there are only minor and ignorable differences in the measurements. Inclusion of the reinforcement reduced the SA values by 8%. On the other hand, the measured period values slightly increases due to the reinforcement effect. The period values at A8 and A9 are 0.04 seconds in the unreinforced model but the period value increases to 0.09 seconds for the reinforced case. Table 4 represents the measured displacement values of embankment models. The geotextile reinforcement application was capable of mitigating the amount of measured displacement values except the toe of the embankment. The measurement of D2 increased slightly in the reinforced case. It is seen that horizontal displacement values between the second reinforcement layer and the crest reduced by 59% in the reinforced model.

Table 4 Displacement values under the Düzce Earthquake Excitations.

Displacement No.	Unreinforced (cm)	Reinforced (cm)
D1	0.98	0.98
D2	0.75	0.88
D3	0.97	0.90
D4	0.49	0.20

Fig. 7 reveals the amplification behaviour of the (U)REM45 models under the Düzce Earthquake excitations. Under the given dynamic motion, A.F. decreases from 1.11 to 0.97 at the crest of the reinforced model which shows that inclusion of the geotextile reinforcement deamplifies the transmitted accelerations.

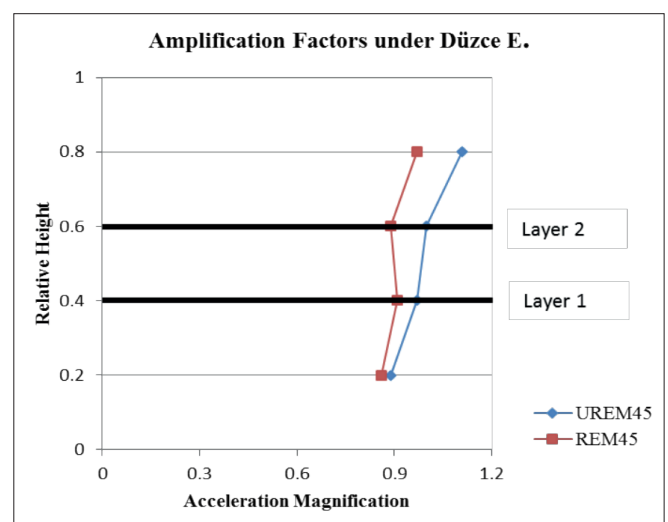


Fig. 7 Amplification factors under Düzce Earthquake Excitations.

3.2 Test results under 0.3g acceleration amplitude

Table 5 represents the PGA values of the UREM and REM under 0.3g acceleration with different frequency levels (Test No. 3–10). Under 0.3g acceleration amplitude, the effect of reinforcement is very limited for the measurements of A2, A3, A4 and A5. The effect of reinforcement at A6 is noticeable only for frequencies of 5Hz and 7Hz. The reduction of the transmitted acceleration values at A8 and A9 equals to 20% under a dominant frequency of 2Hz. It is determined that A.F. decreased from 1.1 to 0.9 at the top of the reinforced embankment model.

Table 5 Acceleration values of (U)REM embankments under 0.3g acceleration amplitude

	2Hz		5Hz		7Hz		14Hz	
	U. (g)	R. (g)	U. (g)	R. (g)	U. (g)	R. (g)	U. (g)	R. (g)
A1	0.30	0.30	0.30	0.30	0.30	0.30	0.30	0.30
A2	0.28	0.30	0.28	0.28	0.29	0.29	0.20	0.32
A3	0.27	0.25	0.25	0.21	0.27	0.26	0.23	0.23
A4	0.28	0.31	0.28	0.27	0.29	0.29	0.28	0.29
A5	0.28	0.32	0.29	0.27	0.29	0.30	0.28	0.28
A6	0.30	0.31	0.41	0.27	0.40	0.30	0.31	0.28
A7	0.35	0.31	0.45	0.28	0.42	0.32	0.38	0.26
A8	0.32	0.26	0.47	0.22	0.47	0.24	0.43	0.22
A9	0.33	0.27	0.54	0.24	0.57	0.26	0.47	0.25

The reduction of the transmitted acceleration values under 0.3g acceleration with a dominant frequency of 5Hz is higher. A7 and A9 measurements decreased by 34% and 56%, respectively. It is seen that reduction ratios tend to increase with respect to the increased height of the embankment. In addition, the maximum A.F. of 1.8 for the unreinforced model decreased to 0.8 for the reinforced model (Fig. 14). Similar dynamic behaviour trend is observed under 0.3g acceleration with 7Hz of frequency. Reinforcement effect decreased the transmitted acceleration values by 54%, from 0.57g to 0.26g at A9. Moreover, A.F. close to the crest decreased from 1.9 to 0.87 for the reinforced embankment model.

Under the dynamic motion of 0.3g acceleration with a dominant frequency of 14Hz, reinforcement effect is clear at A8 and A9. The acceleration measurements of A8 were reduced by 49% in the reinforced model. A9 measurements decreased from 0.47g to 0.25g in the reinforced case which equals to a reduction in acceleration values of 47%. Based on the findings, acceleration-time histories of the UREM and REM under an acceleration amplitude of 0.3g and predominant frequencies of 5 Hz and 7 Hz are plotted in Figs. 8 and 9. Observed significant deamplification within the body of embankment and the crest can be seen in Fig. 14.

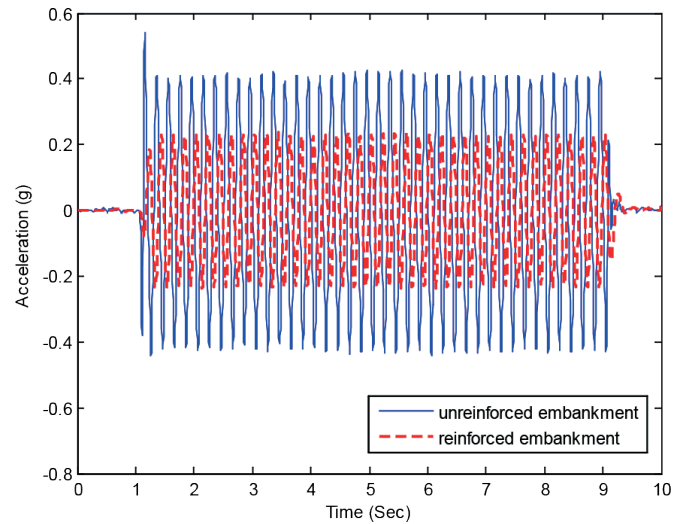


Fig. 8 Acceleration-time histories of UREM and REM under a base acceleration of 0.3g and a frequency of 5Hz (A9).

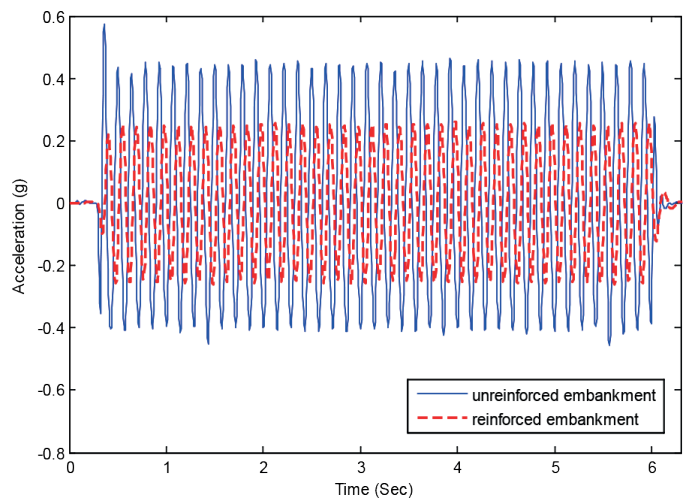


Fig. 9 Acceleration-time histories of UREM and REM under a base acceleration of 0.3g and a frequency of 7Hz (A9).

Table 6 represents the SA and corresponding period values of the UREM and REM under a sinusoidal base acceleration of 0.3g, respectively.

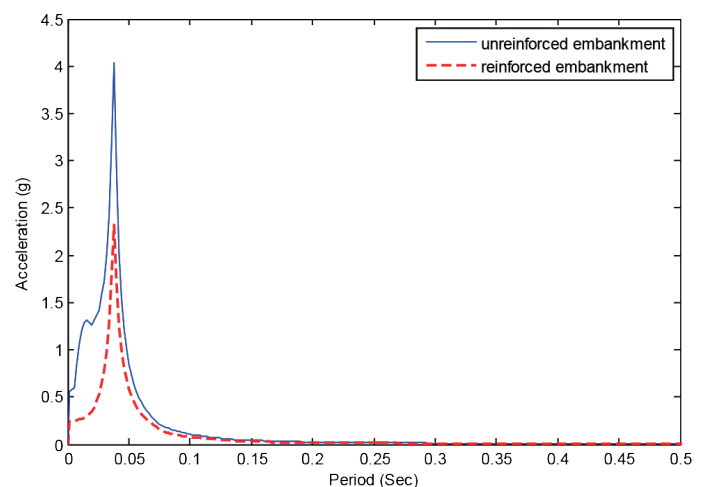


Fig. 10 Response Spectrum under 0.3g acceleration and 5Hz frequency for UREM and REM (A9).

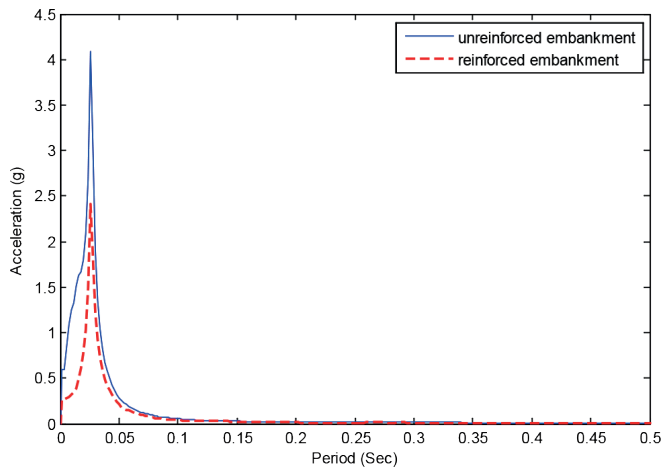


Fig. 11 Response Spectrum under 0.3g acceleration and 7Hz frequency for UREM and REM (A9).

Table 6 SA values of unreinforced and reinforced embankment under 0.3g acceleration.

	2Hz		5Hz		7Hz		14Hz	
	U. (g)	R. (g)	U. (g)	R. (g)	U. (g)	R. (g)	U. (g)	R. (g)
A1	2.83	2.81	2.73	2.73	2.69	2.68	1.94	1.94
A2	2.83	2.82	2.69	2.68	2.87	2.87	1.85	1.86
A3	2.81	2.80	2.64	2.64	2.86	2.85	1.83	1.84
A4	2.82	2.82	2.66	2.66	2.85	2.85	1.82	1.85
A5	2.83	2.82	2.66	2.65	2.87	2.88	1.84	1.84
A6	2.81	2.81	3.75	2.65	3.61	2.83	1.86	1.85
A7	2.85	2.85	3.84	2.71	3.72	2.92	2.15	1.42
A8	2.71	2.53	3.74	2.15	3.73	2.21	2.42	0.53
A9	2.83	2.65	4.04	2.32	4.09	2.41	2.49	0.98

Under 0.3g acceleration and 2Hz dominant frequency, the effect of reinforcement is apparent in the measurements of A8 and A9. SA values decreased up to 7% and this reduction is concentrated at the upper parts of the embankment. Under a dominant frequency of 5Hz, the effectiveness of the geosynthetic increases. SA values decreased up to 43% at the crest (Fig. 10). Similarly, when the reinforced embankment model was subjected to a frequency of 7Hz, SA measurements at the crest decreased up to 41% which is given in Fig. 11.

Results also reveal that SA reduction is better observed under higher predominant frequencies. Under 0.3g acceleration with a frequency motion of 14 Hz, SA values reduced in the range of 34% to 78%. Measured displacement values of the Test No 3-10 are given in Table 7 for UREM and REM.

Table 7 Displacement values of UREM and REM under 0.3g base acceleration.

(cm)	2Hz		5Hz		7Hz		14Hz	
	U.	R.	U.	R.	U.	R.	U.	R.
D1	3.50	3.30	0.70	0.67	0.38	0.34	0.05	0.04
D2	2.99	1.99	0.76	0.44	0.50	0.16	0.59	0.58
D3	2.42	1.51	1.58	1.09	0.86	0.38	0.82	0.85
D4	0.23	0.15	0.98	0.15	0.19	0.12	0.41	0.30

Test results reveal that under a predominant frequency of 2Hz, REM deformed around 35% less within the embankment body. By means of settlements, D4 measured a displacement of 0.23cm. With the effect of the reinforcement, it was measured as 0.15cm with a reduction of almost 35%. Under a dominant frequency of 5Hz, displacement values were reduced by up to 42% with the effect of the reinforcement layers. Under current ground excitations, a settlement value of 0.98cm in the unreinforced case was reduced by 85% to 0.15cm in the scaled reinforced case. Geotextile reinforcement is very efficient under a frequency of 7Hz as the horizontal displacement was reduced by 56% at the toe of the embankment, as well as the amount of settlement was reduced by 37% at the crest. The effect of reinforcement is very limited on displacement values under input motion with a 14Hz predominant frequency. Even the displacement value at the crest increases a bit in the reinforced model, settlement measurements are 27% less when compared with the unreinforced case.

Fig. 12 shows the undeformed and deformed shape of the UREM under a base acceleration of 0.3g with a frequency of 2Hz. Fig.13 shows the undeformed and deformed shape of the REM under a 0.3g base acceleration with a frequency of 14Hz.

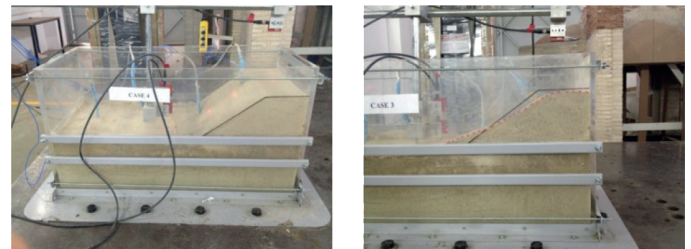


Fig. 12 Undeformed and deformed shape of the UREM under 0.3g acceleration and 2Hz frequency.

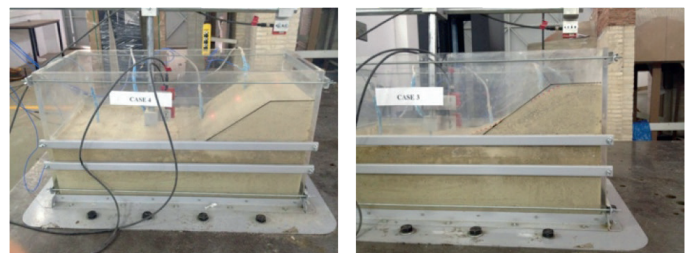


Fig. 13 Undeformed and deformed shape of the REM under 0.3g acceleration and 14Hz frequency.

Fig. 14 gives the amplification behaviour of the (U)REM45 models under a base acceleration of 0.3g. It is seen that the transmitted ground motions passing through geosynthetic layers diminish on REM45 model which creates deamplification. (the left side of the graph) where UREM45 model reflects significant acceleration amplification (the right side of the graph). Reduction of the acceleration amplitudes is more apparent under 5Hz and 7Hz frequencies where the deamplification ratio is over 50%.

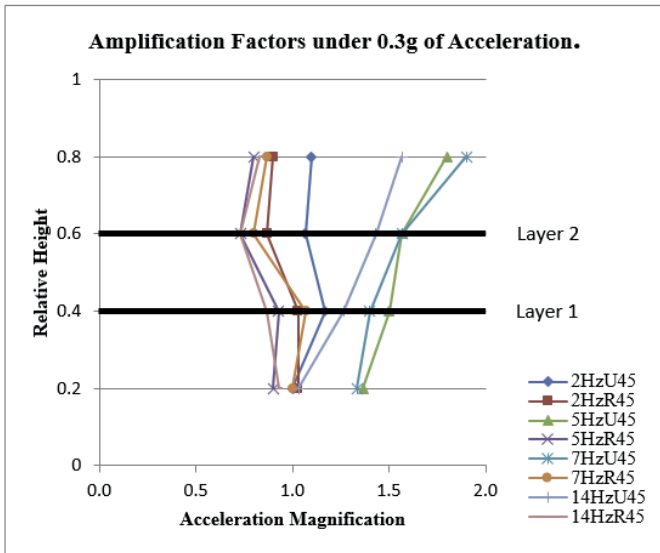


Fig. 14 Amplification Factors of (U)REM45 under 0.3g acceleration.

3.3 Test results under 0.5g acceleration amplitude

Transmitted accelerations, spectral accelerations and displacement values for the 0.5g acceleration amplitude (Test No. 11–18) are represented. Table 8 represents the transmitted acceleration values of the UREM and REM under 0.5g acceleration amplitude for different predominant frequencies.

Table 8 Acceleration values of UREM and REM under 0.5g acceleration amplitude.

	2Hz		5Hz		7Hz		14Hz	
	U. (g)	R. (g)	U. (g)	R. (g)	U. (g)	R. (g)	U. (g)	R. (g)
A1	0.50	0.50	0.50	0.50	0.50	0.50	0.50	0.50
A2	0.40	0.51	0.49	0.49	0.48	0.49	0.49	0.46
A3	0.46	0.40	0.49	0.45	0.45	0.46	0.37	0.34
A4	0.47	0.51	0.50	0.50	0.51	0.50	0.45	0.44
A5	0.47	0.51	0.50	0.50	0.51	0.51	0.45	0.45
A6	0.51	0.50	0.64	0.49	0.63	0.49	0.54	0.45
A7	0.53	0.50	0.66	0.50	0.67	0.50	0.61	0.51
A8	0.53	0.33	0.71	0.34	0.71	0.38	0.77	0.35
A9	0.57	0.34	0.79	0.36	0.76	0.39	0.81	0.39

As can be inferred from Tables, under 0.5g excitation, the transmitted acceleration values are around and close to input excitations at accelerometers A2-A5. As can be seen in Fig. 19, under 2Hz predominant frequency, the reduction ratio of the transmitted accelerations is 40% around the crest where A.F. decreased from 1.14 to 0.68 in the reinforced model under current dynamic motion.

Under 5Hz predominant frequency, the effect of reinforcement is significant at A8 and A9. Due to the inclusion of the reinforcement layers, transmitted accelerations reduced by 55% at the crest (Fig. 15) and similarly A.F. decreased from 1.58 to 0.72. Under 0.5g acceleration with 7Hz predominant frequency, the effectiveness of the reinforcement becomes

clear at the upper part of the embankment model. The amount of reduction in the acceleration values is 46% at A8 and 49% at A9 with transmitted acceleration values of 0.39g (Fig. 14). Also, A.F. value of 1.52 for the UREM decreased to 0.78 for the reinforced model. Under the dynamic motion of 0.5g acceleration with 14Hz predominant frequency, the REM shows the same seismic behaviour trend. Due to the reinforcement the reduction ratio at A6 is 17%, however the reduction ratio at A9 is increased to 52% which is located at the crest and the corresponding A.F. decreased from 1.62 to 0.78. Figs.15 and 16 represent the transmitted acceleration-time histories of the UREM and REM under predominant frequencies of 5Hz and 7Hz for A9, respectively.

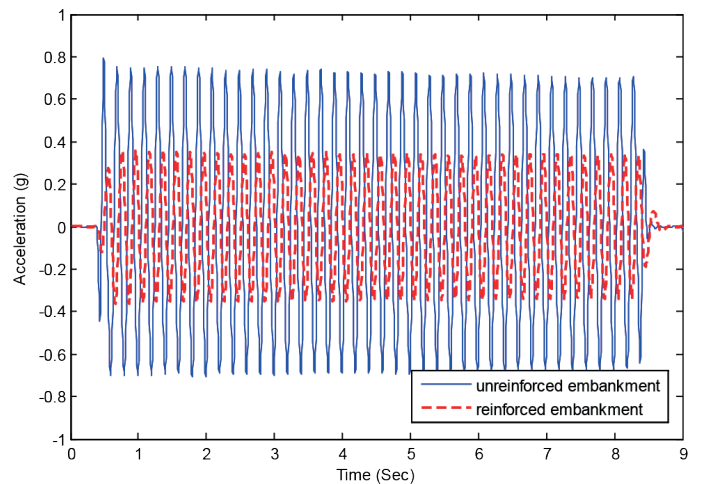


Fig. 15 Acceleration-time histories of UREM and REM under 0.5g acceleration and 5Hz frequency (A9).

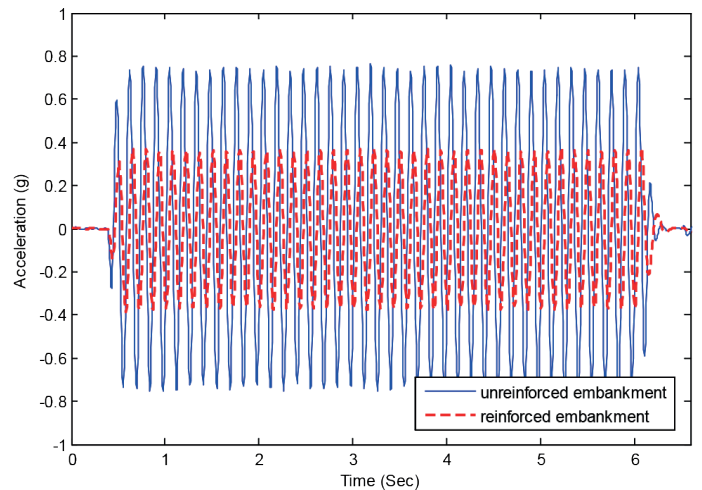


Fig. 16 Acceleration-time histories of UREM and REM under 0.5g acceleration and 7Hz frequency (A9).

Table 9 represents the SA values of the UREM and REM under a base acceleration of 0.5g.

Table 9 SA values of UREM and REM under 0.5g acceleration amplitude.

	2Hz		5Hz		7Hz		14Hz	
	U. (g)	R. (g)	U. (g)	R. (g)	U. (g)	R. (g)	U. (g)	R. (g)
A1	4.54	4.53	4.70	4.71	4.43	4.42	2.75	2.76
A2	4.57	4.57	4.71	4.70	4.46	4.45	2.99	2.99
A3	4.52	4.52	4.71	4.72	4.45	4.44	2.95	2.97
A4	4.59	4.59	4.70	4.71	4.49	4.47	2.92	2.95
A5	4.58	4.57	4.70	4.70	4.50	4.51	2.97	2.98
A6	4.56	4.56	6.13	4.68	5.94	4.45	3.43	2.95
A7	4.61	4.61	6.32	4.83	6.24	4.67	3.85	3.32
A8	4.40	3.10	6.41	3.24	6.59	3.24	4.50	1.92
A9	4.65	3.29	6.83	3.45	7.09	3.48	4.76	2.02

Under 0.5g acceleration amplitude, the effect of reinforcement for the measured SA values is noticeable at the upper portions of the reinforced embankment model. Sensors of A2-A6 that were placed inside the foundation soil measured the similar SA values to the input motion. SA values were reduced by up to 30% under a predominant frequency of 2Hz. Also, under a dominant frequency of 5Hz, the reduction ratio of SA values is up to 50% at A9 (Fig. 17). As seen in Tables, SA values significantly reduce due to the inclusion of the geotextiles. Under a predominant frequency of 7Hz, SA values at the crest were reduced by 51% (Fig. 18). As stated before, reduction ratios of SA values are correlated with the increased frequency ranges. For the base motion with a dominant frequency of 14Hz, SA reduction for the reinforced embankment models was obtained up to 58%.

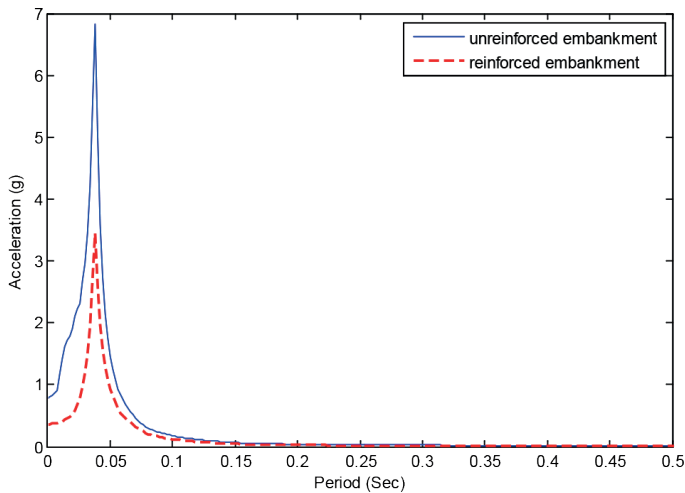


Fig. 17 Response Spectrum under 0.5g acceleration and 5Hz frequency for UREM and REM (A9).

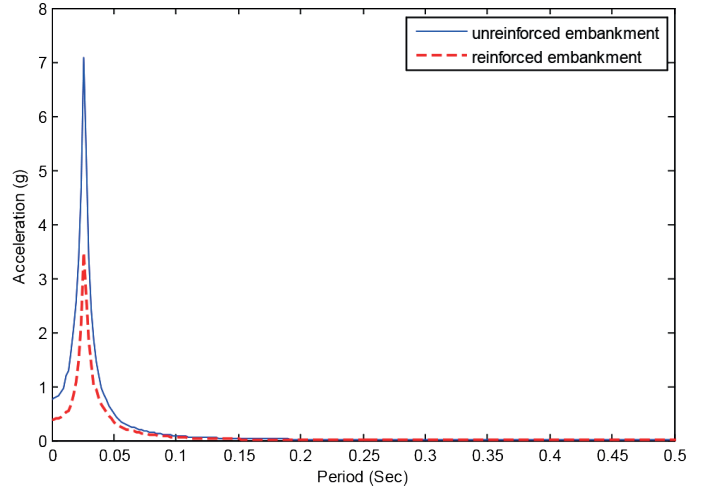


Fig. 18 Response Spectrum under 0.5g acceleration and 7Hz frequency for UREM and REM (A9).

Measured maximum displacement values under 0.5g acceleration amplitude with different predominant frequencies are given in Table 10 for UREM and REM.

Table 10 Displacement values of UREM under base acceleration of 0.5g.

(cm)	2Hz		5Hz		7Hz		14Hz	
	U.	R.	U.	R.	U.	R.	U.	R.
D1	3.49	3.50	0.70	0.70	0.39	0.38	0.05	0.05
D2	3.64	2.99	1.18	0.76	1.42	0.50	0.69	0.59
D3	4.09	2.63	1.29	0.71	0.88	0.45	0.57	0.26
D4	2.10	0.73	0.83	1.91	0.99	0.46	1.60	0.37

Under 0.5g acceleration amplitude with a frequency of 2Hz, the geotextile reinforcement mitigated the amount of displacement value at the top of the embankment around 36%. The settlement measurements by D4 reveal that the reinforcement application reduced the total settlement at the top of the embankment by 65%. Under a frequency of 5Hz, although settlement values increase a bit, the crest of the embankment displaces 45% less in the reinforced model. For the 7Hz frequency, it is seen that due to the geotextile inclusion, measured displacement value at the crest of the embankment was reduced by 65% and vertical displacements were 54% less. Under a frequency of 14Hz, the effect of reinforcement is more effective at the crest of the model. The maximum displacement value at D3 was reduced by 55% in the REM. Moreover, the geotextile reinforcement inclusion impressively mitigates the settlement values. Under the current dynamic loads, the total settlement values were reduced by 77%.

Fig. 19 presents the amplification behaviour of the (U) REM45 models under acceleration amplitude of 0.5g. This Figure clearly reflects the effectiveness of the geotextile reinforcement under high acceleration amplitudes. Especially right after the first reinforcement layer, amplitudes of the transmitted dynamic motions passing through REM45 model substantially diminish and A.F. trends on the graph changes certainly.

It can be said that A.F. reduction is larger under high frequency of motion but the highest reduction is observed under a predominant frequency of 5Hz where A.F. reduction of 54% was observed. Also, the gap between the A.F. trend lines of REM45 model and UREM45 model is at its maximum of this study.

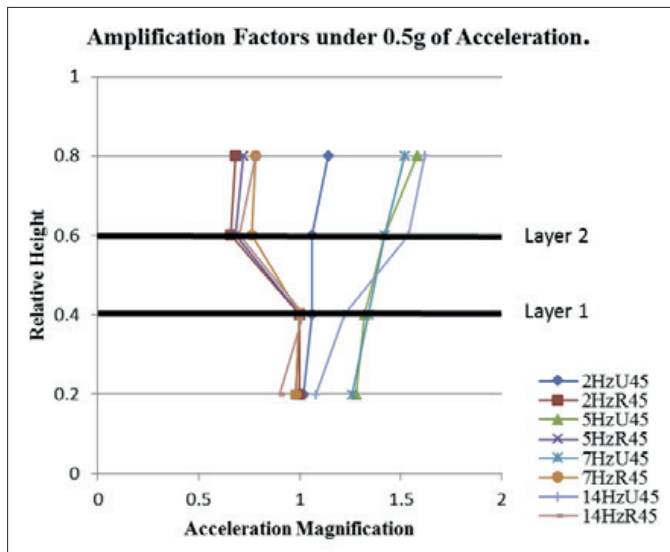


Fig. 19 Amplification Factors of (U)REM45 under 0.5g acceleration.

4 Conclusions

Shake table experiments were performed under nine different dynamic motions including a time scaled real earthquake record and eight sinusoidal base accelerations having two acceleration amplitudes and four predominant frequencies. Conclusions are obtained as follows:

1. The geosynthetic reinforcement application is capable of reducing the transmitted acceleration values up to 56% in the embankment models during shake table tests. The reduction ratio is so much higher around the reinforced zone of the embankment.
2. The effect of reinforcement on seismic performance is very dependent on the acceleration amplitude and frequency content of the dynamic motions.
3. Response spectra indicate that SA values are higher in the unreinforced model. In addition, SA values tend to increase in higher frequency motions.
4. Observed SA values reveal that the reinforcement material is the most effective under the highest frequency of motion which is capable of reducing the SA values up to 78%. The geotextile material is the least effective under scaled earthquake record and under the base acceleration with the lowest predominant frequency motion.
5. Geotextile reinforcement application is quite effective to reduce earthquake induced settlements. Vertical displacement values were reduced by up to 85% in this study.
6. Horizontal displacement values occasionally decrease with the increasing frequency values. Also, the increasing frequency levels cause higher levels of horizontal displacement at

the toe and top of the embankment except the motion with the highest frequency.

7. By means of acceleration amplitude in the shake table experiments, tests under 0.5g acceleration amplitude presents the lower A.F. than the tests with 0.3g acceleration amplitude. In other words, use of geotextile reinforcement is more effective under higher acceleration amplitudes used in this study. Deamplification of the transmitted acceleration values is observed to be greater under frequencies of 5Hz and 7Hz for both amplitudes.

In this study, the benefits of geotextiles are similar to static case where the geotextile carries tensile loads to resist shear failure. As a summary, the experimental study reveals that geotextiles are preferable materials with the tensile capacity of the reinforcement layers. Geotextiles can successfully and effectively mitigate the earthquake hazards and lessen earthquake induced damages. It is seen that the input dynamic motion deamplifies travelling from foundation soil through the reinforced embankment models. So that, the geotextile reinforced highway embankments perform better and remain more stable during the dynamic motions. It is revealed that the efficiency of the geotextile reinforcement is highly dependent on the characteristics of the dynamic motions. Based on the findings of this study, it is recommended that the highway embankments should be designed with respect to the expected earthquake characteristics.

References

- [1] Yegian, M. K., Kadakal, U., Catan, M. "Geosynthetics for earthquake hazard mitigation". In: *Geosynthetics '99: Specifying Geosynthetics and Developing Design Details*. 1, pp. 87–100. 1999.
- [2] Edinçliler, A., Güler, E. "Geotextile-reinforced embankments on soft clays - effects of a foundation soil cruststrengthened by lime diffusion". *Geosynthetics International*, 6(2), pp. 71–91. 1999. <https://doi.org/10.1680/gein.6.0144>
- [3] Edinçliler, A. "Using waste tire-soil mixtures for embankment construction". In: *Proceedings and Monographs in Engineering, Water and Earth Sciences*, International Workshop on Scrap Tire Derived Geomaterials. International Workshop on Scrap Tire Derived Geomaterials. Yokosuka, Japan. Mar. 23–24, 2007, pp. 319–328. 2008.
- [4] Edinçliler, A., Baykal, G., Saygılı, A. "Influence of different processing techniques on the mechanical properties of used tires in embankment construction". *Waste Management*, 30(6), pp. 1073–1080. <https://doi.org/10.1016/j.wasman.2009.09.031>
- [5] Koerner, R. M. "Designing with geosynthetics". Pearson Education, Inc, Upper Saddle River, NJ, USA. 2005.
- [6] El-Emam, M. E., Bathurst, R. J. "Experimental design, instrumentation and interpretation of reinforced soil wall response using a shaking table". *International Journal of Physical Modeling in Geotechnics*, 4(4), pp. 13–32. 2004. <https://doi.org/10.1680/ijpmg.2004.040402>
- [7] El-Emam, M. E., Bathurst, R. J. "Influence of reinforcement parameters on the seismic response of reduced-scale reinforced soil retaining walls". *Geotextiles and Geomembranes*, 25(1), pp. 33–49. 2007. <https://doi.org/10.1016/j.geotextmem.2006.09.001>
- [8] Iai, S. "Similitude for shaking table tests on soil-structure fluid model in 1-g gravitational field". *Soils and Foundations*, 29(1), pp. 105–118. 1989.

- [9] Perez, A., Holtz, R. D. "Seismic response of reinforced steep soil slopes: results of shaking table study". In: *Geotechnical Engineering for Transportation Projects*, (Yegian, M. K., Kavazanjian, E. (Eds.)) pp. 1664–1672. ASCE, 2004. <https://doi.org/10.1061/9780784407448>
- [10] Wartman, J., Seed, R. B., Bray, J. D. "Shaking table modeling of seismically induced formations in slopes". *Journal of Geotechnical and Geoenvironmental Engineering*, 131(5), pp. 610–622. 2005. [https://doi.org/10.1061/\(ASCE\)1090-0241\(2005\)131:5\(610\)](https://doi.org/10.1061/(ASCE)1090-0241(2005)131:5(610))
- [11] Lin, M. L., Wang, K. L. "Seismic behavior in a large-scale shaking table test". *Engineering Geology*, 86(2–3), pp. 118–133. 2006. <https://doi.org/10.1016/j.enggeo.2006.02.011>
- [12] Srilatha, N., Latha, G. M., Puttappa, C. G. "Effect of frequency on seismic response of reinforced soil slopes in shaking table tests". *Geotextiles and Geomembranes*, 36, pp. 27–32. 2013. <https://doi.org/10.1016/j.geotextmem.2012.10.004>
- [13] Yang, K., Zornberg, J., Liu, C., Lin, H. "Backfill stress and strain information within a centrifuge geosynthetic-reinforced slope model under working stress and large soil strain conditions". In: *GeoCongress 2012: State of the Art and Practice in Geotechnical Engineering*. pp. 461–470. 2014. <https://doi.org/10.1061/9780784412121.048>
- [14] Aklik, P., Wu, W. "Centrifuge model tests on foundation on geosynthetic reinforced slope". Proceedings of the 18th International Conference on Soil Mechanics and Geotechnical Engineering, Sep. 2–6. Paris, France. 2013,
- [15] Yang, K. H., Hung, W.Y., Kencana, E.Y. "Acceleration-amplified responses of geosynthetic-reinforced soil structures with a widerange of input ground accelerations". In: *Geo-Congress 2013: Stability and Performance of Slopes and Embankments III*. (Meehan, C., Pradel, M. A., Éabuz, J. F. (Eds.)) Mar. 3–7. San Diego, California, United States. 2013. <https://doi.org/10.1061/9780784412787.119>
- [16] Harris, H. G., Sabnis, G. M. "Structural modeling and experimental techniques". CRC Press, New York. 1999.
- [17] Cihan, K., Yuksel, Y. "Deformation of breakwater armored artificial units under cyclic loading". *Applied Ocean Research*, 42, pp. 79–86. 2013. <https://doi.org/10.1016/j.apor.2013.05.002>
- [18] Harris, D. W., Snorteland, N., Dolen, T., Travers, F. Shaking table 2D models of a concrete gravity dam. *Earthquake Engineering & Structural Dynamics*, 29(6), pp. 769–787. 2000.
- [19] Akay, O., Özer, A. T., Fox, G. A., Bartlett, S. F., Arellano, D. "Behavior of sandy slopes remediated by EPS-block geofom under seepage flow". *Geotextiles and Geomembranes*, 37, pp. 81–98. 2013. <https://doi.org/10.1016/j.geotextmem.2013.02.005>
- [20] Taylor, C. A., Dar, A. R., Crewe, A. J. (1996) "Shaking table modeling of seismic geotechnical problems." In: *Proceedings of the 10th European Conference on Earthquake Engineers*, Vienna, Austria. 1, pp. 441–446. 1995.
- [21] Toksoy, Y. S. "Investigation of the seismic performance of reinforced highway embankments." M.Sc. Thesis, Boğaziçi University, Istanbul, Turkey. 2014.
- [22] Çağatay, A. (2008) "Investigation of the effect of tire waste inclusions on the shear strength parameters of sand." M.Sc. Thesis, Boğaziçi University
- [23] Bathurst, R. J., Hatami, K. "Seismic Response Analysis of a Geosynthetic-Reinforced Soil Retaining Wall". *Geosynthetics International*, 5(1–2), pp. 127–166. 1998. <https://doi.org/10.1680/gein.5.0117>